Purinergic Signalling (2005) 1: 271–280
DOI: 10.1007/s11302-005-0650-8

Identification of a tyrosine residue responsible for *N*-acetylimidazole-induced increase of activity of ecto-nucleoside triphosphate diphosphohydrolase 3

Saswata Basu & Terence L. Kirley
Department of Pharmacology and Cell Biophysics, University of Cincinnati, Cincinnati, Ohio, USA

Received 19 November 2004; accepted in revised form 15 December 2004

Key words: acetylation, *N*-acetylimidazole, NTPDase3, nucleoside triphosphate diphosphohydrolase, oligomeric structure, site-directed mutagenesis, tyrosine modification

Abstract

Chemical modification in combination with site-directed mutagenesis was used to identify a tyrosine residue responsible for the increase in ecto-nucleoside triphosphate diphosphohydrolase 3 (NTPDase3) nucleotidase activity after acetylation with a tyrosine-selective reagent, *N*-acetylimidazole. The NTPDase3 ATPase activity is increased more than the ADPase activity by this reagent. Several fairly well conserved tyrosine residues (252, 255, and 262) that are located in or very near apyrase conserved region 4a (ACR4a) were mutated. These mutants were all active, but mutation of tyrosine 252 to either alanine or phenylalanine eliminated the activity increase observed after *N*-acetylimidazole treatment of the wild-type enzyme. This suggests that the acetylation of tyrosine 252 is responsible for the increased activity. Stabilization of quaternary structure has resulted in increased enzyme activities for the NTPDases. However, mutation of these three tyrosine residues did not result in global changes of tertiary or quaternary structure, as measured by Cibacron blue binding, chemical cross linking, and native gel electrophoretic analysis. Nevertheless, disruption of the oligomeric structure with the detergent Triton X-100 abolished the increase in activity induced by this reagent. In addition, mutations that abolished the *N*-acetylimidazole effect also attenuated the increases of enzyme activity observed after lectin and chemical cross-linking treatments, which were previously attributed to stabilization of the quaternary structure. Thus, we speculate that the acetylation of tyrosine 252 might induce a subtle conformational change in NTPDase3, resulting in the observed increase in activity.

Abbreviations: ACR – apyrase conserved region; BSA – bovine serum albumin; Con A – Concanavalin A; DMEM – (Dulbecco's modified Eagle medium); DMSO – dimethyl sulfoxide; DSS – disuccinimido suberate; DTT – (dithiothreitol); MOPS – (3-[*N*-morpholino] propanesulfonic acid; *N*-AI – *N*-acetylimidazole; NTPDases – (nucleoside triphosphate diphosphohydrolases); Pi – (inorganic phosphate); PVDF – polyvinylidene fluoride; TBS – (tris buffered saline)

Introduction

The eNTPDases are a family of enzymes that hydrolyze extracellular nucleoside 5′ di- and triphosphates in the presence of divalent cations [1]. There are integral membrane protein NTPDases, embedded in both the cell surface membrane and internal membranes, as well as NTPDases that can be secreted extracellularly as soluble nucleotidases [2–7]. Four of the eight human NTPDases described to date (NTPDase1–3, 8) are integral membrane, cell-surface glycoproteins, with large extracellular domains and two transmembrane domains located near the N- and C-termini [1, 8].

Correspondence to: Dr Terence L. Kirley, Department of Pharmacology and Cell Biophysics, University of Cincinnati College of Medicine, 231 Albert Sabin Way, Cincinnati, OH 45267-0575, USA. Tel: +1-513-558-2338; Fax: +1-513-558-1169; E-mail: terry.kirley@uc.edu

Several areas of sequence conservation in the NTPDases have been noted. Besides the four apyrase conserved regions (ACRs) originally described [9], and ACR5 described later [10, 11], there are also two other conserved protein motifs in the NTPDases that have been named ACR1a and ACR4a [12]. No amino acid residues in the ACR1a region have thus far been assigned any functional significance. However, ACR4a was found to include a conserved glycine residue (glycine 263 in NTPDase3 [12]) whose mutation to alanine caused complete inactivation of the enzyme, presumably by large-scale disruption of native tertiary and quaternary structures of the nucleotidase [12]. A similar, but slightly less pronounced effect was found by mutation of another conserved glycine residue to alanine in NTPDase3, i.e., glycine 462, located in ACR5 [12].

The enzymatic activities, and therefore presumably the physiological functions, of the cell-surface NTPDases are dependent on their oligomeric state (quaternary structure).

Conditions that stabilize NTPDase homo-oligomers increase activity, while conditions that destabilize NTPDase oligomers decrease nucleotidase activities [13]. For example, solubilization with Triton X-100 detergent disrupts the native oligomeric structure and dramatically decreases nucleotidase activities for both NTPDase1 (CD39 [14]) and NTPDase3 [15]. Lectins such as the tetravalent Con A protein can induce lattices of specific glycoproteins, even in the presence of complex mixtures of glycoproteins exposed to Con A [16]. Thus, several studies have reported that Con A increases NTPDase activity [17–19], presumably by stabilization of the quaternary structure. At least in NTPDase3, this Con A effect seems to be mediated via the conserved N81 glycosylation site, located near ACR1 [20]. It has also been shown that chemical cross-linking can stabilize quaternary structure, and therefore the lysine specific cross-linking agent, DSS, has been used to assess possible changes in quaternary structure as a consequence of site-directed mutagenesis of NTPDase3 [12, 21–24]. Of course, the enzymatic activities of the NTPDases are also dependent on their tertiary structures. Cibacron blue (Reactive Blue 2) is a triazine dye that has affinity for the nucleotide binding site of many proteins, and has been shown to inhibit nucleotide handling enzymes in general [25, 26], as well as specific NTPDases [27, 28]. Cibacron blue binding to NTPDase3 is retained after solubilization and monomerization with Triton X-100 [12]. As a consequence, this dye has been used as a measure of native tertiary structure for NTPDase3, since it does not bind to heat-denatured NTPDase3 or to certain mutants that appear to have disrupted tertiary structures [29].

While screening chemical modification reagents for effects on NTPDase3 nucleotidase activities, we made the unusual and unexpected observation that reaction of wild-type NTPDase3 with the tyrosine selective reagent, *N*-acetylimidazole, increases enzyme activity. Previously, treatment with aspirin (acetylsalicylic acid) was shown to inhibit rat platelet NTPDase [30], possibly via acetylation. In the present study, it seems unlikely that an increase in NTPDase3 activity would be induced by acetylation of an active site residue by *N*-acetylimidazole. Therefore, we mutated several conserved tyrosine residues in the vicinity of the glycine residue that was previously proposed to be important for NTPDase3 higher-order structure (glycine 263 in ACR4a [12]). These tyrosine residues are also located near the computer-predicted helix–loop–helix dimerization domain in the primary structure of NTPDase3 (^{238}NTSDIMQVS^{246} [31]).

We found that substitution of tyrosine at position 252 abolished the increase in activity caused by *N*-acetylimidazole, suggesting that modification of this tyrosine residue is responsible for the increased activity of the wild-type enzyme. Monomerization of the wild-type enzyme by solubilization with the detergent Triton X-100 eliminated the increase in activity upon treatment with *N*-acetylimidazole. However, no gross changes in the tertiary or quaternary structures were detected by Cibacron blue binding, DSS cross-linking, or native gel electrophoresis. Nevertheless, changes in response to lectin and cross-linking induced increases in nucleotidase activities were evident in the mutants non-responsive to *N*-acetylimidazole. Therefore, we speculate that Tyr 252, as well as the amino acid residues nearby Tyr 252 in ACR4a, may be important for full enzymatic activity of NTPDase3 due to their subtle influence on native tertiary and/or quaternary structure.

Materials and methods

Materials

The QuikChange™ site-directed mutagenesis kit was purchased from Stratagene. Oligonucleotides were synthesized by the DNA Core Facility at the University of Cincinnati. Lipofectamine Plus Reagent, Dulbecco's modified Eagle medium (DMEM), calf serum, and antibiotics/antimycotics were obtained from Gibco/Life Technologies. The mammalian expression vector pcDNA3 was obtained from Invitrogen. The chemical cross-linking reagent disuccinimidyl suberate (DSS) and the SuperSignal chemiluminescence reagents were purchased from Pierce Chemical Company. Cibacron Blue Gel (Affi-Gel Blue), pre-cast SDS-PAGE 4%–15% gradient mini-gels, and goat anti-rabbit horseradish peroxidase conjugated secondary antibody were obtained from Bio-Rad Laboratories. *N*-Acetylimidazole (*N*-AI), Ampicillin, nucleotides, and other reagents were from Sigma.

Site-directed mutagenesis of NTPDase3

Mutagenesis of NTPDase3 in pcDNA3 vector was performed using the Quick Change site-directed mutagenesis kit (Stratagene) as described previously [12, 15, 23, 24, 29, 32]. The sense nucleotides used for mutagenesis are as follows:

Y252A, 5′-CTGTATGGCTACGTAGCAACGCTCTACACACAC-3′;
Y255A, 5′-TACGTATACACGCTCGCAACACACAGCTTCCAG-3′;
Y262A, 5′-CACAGCTTCCAGTGCGCAGGCCGGAATGAGGCT-′3;
Y252F, 5′-TATGGCTACGTATTCACGCTCTACACA-3′;
Y255F, 5′-GTATACACGCTCTTCACACACAGCTTC-3′;
Y262F, 5′-AGCTTCCAGTGCTTTGGCCGGAATGAG-′3;

Altered codons are underlined, but the complementary antisense oligonucleotides also necessary for mutagenesis are not shown. The presence of the desired mutation and lack of undesired mutations were confirmed by DNA sequencing. The mutated NTPDase3 cDNA was used to transform competent cells as described by the manufacturer (Stratagene).

Transient transfection

COS-1 cells were grown and transfected with wild-type and mutant NTPDase3 cDNA, as previously described

[12, 15, 23, 24, 29, 32]. An empty pcDNA3 vector was transfected into COS cells and used as a background control for nucleotidase assays. Cells were harvested 48 h post-transfection and crude total membrane preparations were obtained as described [12, 15, 23, 24, 29, 32].

Protein assay

Protein concentrations were determined using the Bio-Rad Coomassie blue dye binding assay, using bovine serum albumin as the standard, with the modifications of Stoscheck [33].

Nucleotidase assays

Nucleotidase activities were determined by measuring the concentration of inorganic phosphate (P_i) released from the ATP or ADP substrates in the presence of Mg^{2+} or Ca^{2+}. Assays were performed at 37 °C as previously described [12, 15, 23], modified from Fiske and Subbarow [34]. Nucleotidase activities were corrected for COS-1/pcDNA3 background (provided by the empty pcDNA3 vector transfected into COS-1 cells) and for differences in expression levels relative to those of wild-type, as determined by Western blotting.

Western blot analysis

For Western blot, proteins were resolved in a 4%–15% linear gradient SDS-PAGE gradient gel (BioRad 4–15%) and transferred to a polyvinylidene fluoride (PVDF) membrane. Blots were probed with an anti-C-terminal peptide NTPDase3 antibody, as previously described [32].

Chemical cross-linking

COS cell membrane preparations (at a total protein concentration of 0.1 mg/ml) were diluted in 20 mM MOPS, 5 mM $MgCl_2$ buffer, pH 7.4, and incubated for 20 min at 22 °C with 200 μM disuccinimido suberate (DSS) freshly dissolved in DMSO. Non-cross-linked samples were treated with the same volume of DMSO, and the final DMSO concentration of all samples was less than 2% of the total sample volume. The cross-linking reaction was stopped by incubation with an excess (10 mM) of lysine for 5 min at 22 °C. Samples were then either analyzed for intermolecular cross-linking by reducing SDS-PAGE and Western blot analysis, or assayed for Mg^{2+}-ATPase activity as described above.

Analysis of Cibacron blue binding

Cibacron blue binding assays have been described previously [12, 23, 29].

Native gel electrophoresis of wild-type and mutant NTPDases

NTPDase3 membrane preparations were solubilized for 10 min at room temperature in digitonin (1% final concentration), a detergent known to preserve the native quaternary structure and the activity of the NTPDases [13, 14]. Soluble proteins were isolated by centrifugation and run on 6% Laemmli native gel containing 0.1% digitonin as described previously [12].

Treatment of wild-type and mutant NTPDase3 with Concanavalin A

Concanavalin A (Con A) was prepared at a concentration of 5 mg/ml in 20 mM MOPS buffer containing 100 mM NaCl, 1 mM $MnCl_2$ and 1 mM $CaCl_2$, pH 7.4. Wild-type and tyrosine mutant NTPDase3 total membrane preparations (2 μg) were incubated with 5 μl of 5.0 mg/ml Con A at 37 °C for 15 min before the addition of substrate. Nucleotidase assays were performed in the presence of 5 mM Ca^{2+} or Mg^{2+}, at a final nucleotide concentration of 2.5 mM.

N-acetylimidazole treatment

Membrane preparations were diluted to a total protein concentration of 0.1 mg/ml in pH 7.4 MOPS buffer containing 5 mM $MgCl_2$. At 0 time (before addition of *N*-acetylimidazole) 20-μl aliquots were diluted into 260 μl of an ice-cold stop solution containing an excess of lysine (14.5 mM) to quench the reaction, 100 mM KCl, 5 mM $MgCl_2$, 1 mM EGTA and 20 mM Tris–HCl, pH 7.0. *N*-Acetylimidazole (2 mM) was then added to the remainder of each membrane preparation at 22 °C. At 5, 10, 20, 30, 45 and 60 min, 20 μl aliquots were diluted with 260 μl of stop solution as described above. At 61 min, hydroxylamine was added to a final concentration of 200 mM to the remainder of the *N*-acetylimidazole-treated membrane preparation to quench the reaction and reverse the acetylation of tyrosine residues. At 62, 65, 75, 90 and 120 min, 21-μl aliquots were diluted with 259 μl stop solution as before. Mg^{2+}-ATPase and Mg^{2+}-ADPase assays were performed for all time points.

Time dependence of Mg-ATPase activity

Kinetics of Mg^{2+}-dependent ATPase hydrolysis before and after treatment with *N*-acetylimidazole or the lysine-specific cross linker, DSS, were measured in a Beckman DU-800 spectrophotometer, using a NADH-linked-enzyme spectrophotometric assay [35], as described previously for NTPDase2 [22] and NTPDase3 [20]. The NADH-linked-enzyme assay was used to allow the continuous monitoring of ATPase activity as a function of time. After pre-incubation to bring the cuvettes and samples to 37 °C, the

Table 1. Multiple sequence alignments of extended NTPDase ACR4a regions.

eNTPDase	Species	Accession no.	Amino acid sequence
NTPDase3	Human	AF034840	250 YV**Y**TL**Y**THSFQC**Y** *G*RNEA
	Rat	NP_835207	250 YV**Y**TL**Y**THSFQC**Y** *G*RNEA
	Mouse	AY376710	250 YV**Y**TL**Y**THSFQC**Y** *G*RNEA
NTPDase2	Human	Q9Y5L3	231 QH**Y**RV**Y**THSFLC**Y** *G*RDQV
	Rat	O35795	231 QH**Y**RV**Y**THSFLC**Y** *G*RDQI
	Chicken	P79784	228 QP**Y**KV**Y**THSFLC**Y** *G*RDQV
NTPDase1	Human	P49961	244 KD**Y**NV**Y**THSFLC**Y** *G*KDQA
	Mouse	P55772	243 ED**Y**TV**Y**THSFLC**Y** *G*KDQA
	Pig	Q9MYU4	244 KN**Y**SV**Y**THSFLC**Y** *G*KDQA
NTPDase8	Mouse	AY3644442	237 AN**Y**SV**Y**THSYLCF *G*RDQI
NTPDase4	Human	AF016032	309 HV**Y**RV**Y**VATFLGF *G*GNAA
NTPDase7	Human	AF269255	309 HV**Y**RV**Y**VTTFLGF *G*GNFA
NTPDase5	Human	AF039918	233 ST**Y**KL**Y**THSYLGF *G*KAAA
NTPDase6	Human	AF039916	285 RT**Y**KL**Y**SYSYLGL *G*LMSA

The sequence alignment shows the region near apyrase conserved region 4a (ACR4a). The three tyrosine residues mutated in this work (human NTPDase3 Y252, Y255, and Y262) are in bold and underlined in the aligned ACR4a sequences. The conserved glycine residue in ACR4a previously shown to be important for the structure of NTPDase3 (G263, [12]) is italicized and double-underlined. Although only a few representative sequences of the NTPDases are shown in the table, it should be noted that residues corresponding to tyr252 and tyr255 in NTPDase3 are conserved in all NTPDase sequences determined to date.

reactions were initiated by addition of a small volume of NTPDase3 enzyme.

Solubilization and nucleotidase assays

Cell membranes (at a total protein concentration of 0.1 mg/ml) were solubilized in 1% Triton X-100, 5 mM $MgCl_2$ and 20 mM MOPS buffer pH 7.4 at 22 °C for 10 min with occasional mixing, followed by centrifugation at 150,000 *g* for 30 min at 22 °C. Mg^{2+} and Ca^{2+} ATPase and ADPase activities were measured in presence of 0.1% Triton X-100, after adding nucleotide to a final nucleotide concentration of 0.435 mM, using a malachite green phosphate assay [36] to measure nucleotidase activities, since Triton X-100 causes turbidity in the modified Fiske and Subbarow assay [34].

Results

Rationale for selection and analysis of tyrosine mutants

We mutated several tyrosine residues (Tyr 252, 255, and 262) in the vicinity of a computer predicted, myc-type, helix–loop–helix dimerization domain (^{238}NTSDIMQVS [31]), which is also nearby a region of the enzyme (ACR4a) previously identified as containing a glycine residue important for folding or structure of NTPDase3 (Gly 263 [12], see Table 1). Tyrosines corresponding to residues 252 and 255 in NTPDase3 are conserved in all NTPDases, while the tyrosine analogous to tyrosine 262 in NTPDase3 is conserved in the cell-surface membrane NTPDases (NTPDase1, 2, and 3), but not in the other NTPDases (see Table 1). Besides the sequence conservation and the location of the tyrosine residues, another reason for analyzing these mutations was suggested by the unusual experimental observation that *N*-acetylimidazole, a tyrosine selective chemical modification reagent, caused an increase in enzymatic activity of wild-type NTPDase3 (Figures 1 and 2). We hypothesized that modification of one or more of these tyrosine residues might be responsible for the increased enzyme activity.

Protein expression levels

Expression levels of the NTPDase3 mutants were calculated by quantification of Western blots as previously described [12] and compared to wild-type NTPDase3 using an Alpha Innotech FluorChem 8800 Imager. The values presented are the average of three separate transfections (Table 2), and the specific activities for ATP and ADP of the NTPDase3 mutants were corrected for variations in expression levels relative to those of the wild-type (see Table 2).

Nucleotidase activities of NTPDase3 mutants

ATPase and ADPase nucleotidase activities of all mutants were determined in the presence of either Mg^{2+} or Ca^{2+} (Table 2). All tyrosine mutants were active and displayed nucleotidase activities similar to the wild-type NTPDase3, with expression levels 52%–85% of the wild-type NTPDase3 (Table 2). One difference noted is the increased Mg^{2+}-ADPase activity of the Y255A (182%) and Y255F (170%) mutants, relative to the wild-type.

N-acetylimidazole increases Mg^{2+}-ATPase/ADPase activity

N-acetylimidazole increases both ATPase and ADPase activity of wild-type NTPDase3 in presence of Mg^{2+}. After 60 min of reaction, Mg^{2+}-ATPase and Mg^{2+}-ADPase activities are increased by approximately 1.9-fold (Figures

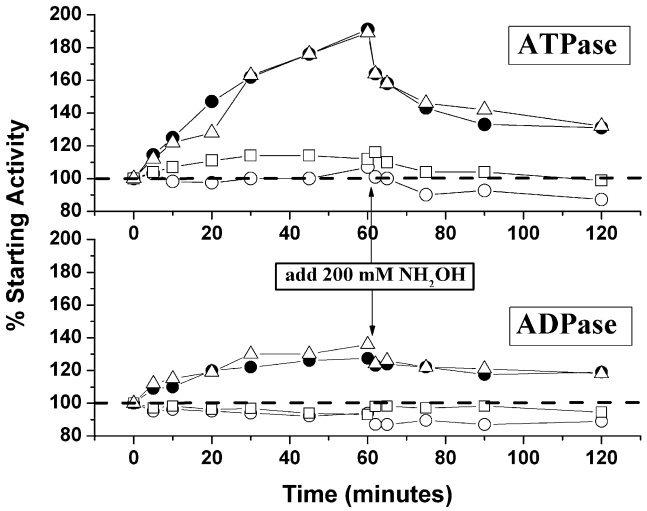

Figure 1. N-acetylimidazole increases NTPDase3 Mg^{2+}-ATPase and Mg^{2+}-ADPase activities of wild-type and Y262A mutants, but not Y252A or Y255A mutants. Mutants [Y252A (○), Y255A (□), and Y262A (△)] and wild-type NTPDase3 (●) COS cell membrane preparations were incubated with *N*-acetylimidazole for various times, and the reaction was terminated by dilution into stop solution as described in Materials and methods. Nucleotidase assays were performed in the presence of 5 mM Mg^{2+}, at a final nucleotide concentration of 2.5 mM. Top panel: ATPase activities. Bottom panel: ADPase activities. Hydroxylamine was added to a final concentration of 200 mM at 61 min, to reverse tyrosine modification. All activities are expressed as a percentage of the nucleotidase activities before *N*-acetylimidazole was added.

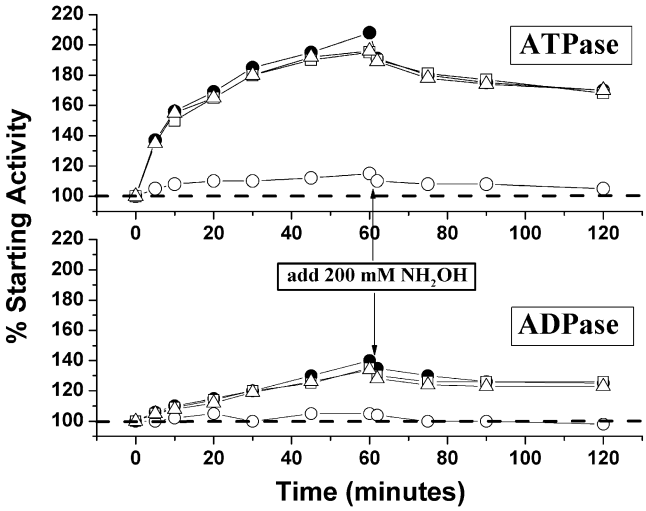

Figure 2. N-acetylimidazole increases NTPDase3 Mg^{2+}-ATPase and Mg^{2+}-ADPase activities of wild-type, Y255F and Y262F mutants, but not the Y252F mutant. Mutants [Y252F (○), Y255F (□), and Y262F (△)] and wild-type NTPDase3 (●) COS cell membrane preparations were incubated with *N*-acetylimidazole for various times, and the reaction was terminated by dilution into stop solution as described in Materials and methods. Nucleotidase assays were performed in presence of 5 mM Mg^{2+}, at a final nucleotide concentration of 2.5 mM. Top panel: ATPase activities. Bottom panel: ADPase activities. Hydroxylamine was added to a final concentration of 200 mM at 61 min, to reverse tyrosine modification. All activities are expressed as a percentage of the nucleotidase activities before *N*-acetylimidazole was added.

1 and 2, upper panels) and 1.35-fold (Figures 1 and 2, lower panels), respectively. A substantial portion of the increase in activity is rapidly reversible by hydroxylamine added at 61 min (Figures 1 and 2), suggesting that tyrosine modification, rather than lysine modification, is responsible for the effect, since tyrosine modification, unlike lysine modification by *N*-AI, is reversible by hydroxylamine. As is evident from Figure 2, *N*-acetylimidazole is unable to increase the nucleotidase activity of the Y252F mutant, in contrast to the wild-type, Y255F, and Y262F mutant NTPDase3. Interestingly, the *N*-acetylimidazole-induced increase is also greatly attenuated in the Y255A mutant, as well as being eliminated in the Y252A mutant (Figure 1).

Kinetics of Mg-ATPase activity after N-acetylimidazole treatment

To investigate the reaction kinetics of Mg^{2+}-ATPase after *N*-acetylimidazole-mediated chemical modification of wild-type NTPDase3, continuous measurement of the Mg-ATPase activity was made using the linked enzyme assay. The data obtained was fit using a double exponential decay function (Figure 3), suggesting two processes causing decreases in enzymatic activity at 37 °C, which occur on different time scales. *N*-Acetylimidazole decreases the rate of decay of activity, resulting in the measured increase in activity (Figures 1 and 2).

Table 2. Nucleotidase activities of wild-type (WT) and mutant NTPDase3 enzymes.

NTPDase3 enzyme	% Wt. level of expression	Normalized Mg^{2+}-ATPase activity (% wt.)	Normalized Ca^{2+}-ATPase activity (% wt.)	Normalized Mg^{2+}-ADPase activity (% wt.)	Normalized Ca^{2+}-ADPase activity (% wt.)
Wild-type	100	144 ± 10 (100)	413 ± 35 (100)	57 ± 5 (100)	83 ± 15 (100)
Y252F	60 ± 5	138 ± 10 (95)	360 ± 30 (87)	48 ± 5 (84)	84 ± 8 (101)
Y255F	85 ± 7	170 ± 12 (118)	397 ± 24 (96)	97 ± 12 (170)	96 ± 10 (115)
Y262F	84 ± 5	158 ± 9 (109)	394 ± 23 (95)	59 ± 8 (103)	84 ± 18 (101)
Y252A	52 ± 6	140 ± 12 (97)	345 ± 36 (83)	51 ± 7 (89)	86 ± 7 (103)
Y255A	67 ± 5	172 ± 15 (119)	392 ± 26 (95)	104 ± 15 (182)	106 ± 10 (127)
Y262A	70 ± 4	159 ± 7 (110)	410 ± 25 (99)	60 ± 12 (105)	85 ± 20(102)

Values given represent the means ± standard deviations of three separate transfections (which were matched to their own wild-type and empty pcDNA3 vector controls). Activities were measured in presence of 5 mM $MgCl_2$ or $CaCl_2$ at a final concentration of 2.5 mM ATP or ADP. Values were normalized for different NTPDase3 protein expression levels by dividing the nucleotidase activity (expressed in the table as μmol Pi/mg protein/h) by the expression level relative to the wild-type enzyme.

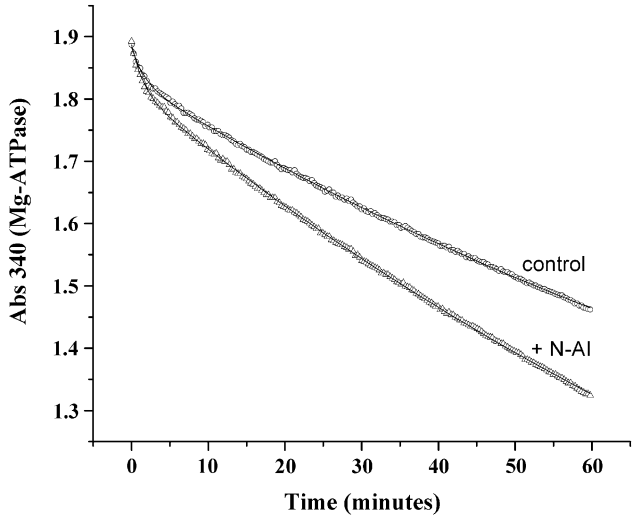

Figure 3. Time dependence of NTPDase3 Mg^{2+}-ATPase activity with and without *N*-acetylimidazole treatment. Wild-type COS cell membrane preparations were treated with water or *N*-acetylimidazole for 60 min and the reaction was terminated by dilution in stop solution as described in Materials and methods. The Mg^{2+}-ATPase activity of 3 μg protein was measured by the NADH-linked enzyme assay [35].

Is N-acetylimidazole modification associated with higher oligomer formation?

To investigate whether the *N*-acetylimidazole modification triggers higher oligomer formation, wild-type NTPDase3 was treated with *N*-acetylimidazole for various times (0, 5, 30, 45 and 60 min) and then run on a native gel. All samples ran with same electrophoretic mobility as untreated NTPDase3, indicating that *N*-acetylimidazole does not initiate higher order oligomer formation as measured by this technique. In addition, the electrophoretic mobilities of wild-type NTPDase3 and the tyrosine mutants are indistinguishable in this native gel electrophoresis, suggesting that the mutants have the same gross oligomeric structure as wild-type NTPDase3. Also, a lysine-specific cross-linking agent, disuccinimido suberate (DSS), was used to assess gross changes in quaternary structure. After reducing SDS-PAGE and Western blotting, wild-type and all NTPDase3 mutants made in this study were similarly cross-linked into dimers, suggesting that the gross quaternary structures of the mutants are similar to those of the wild-type (all data mentioned above is not shown due to lack of demonstrable differences between the wild-type and mutant enzymes).

Table 3. Effect of Triton X-100 solubilization on *N*-acetylimidazole stimulation of wild-type NTPDase3 Mg^{2+}-ATPase activity.

Treatment	Mg^{2+}-ATPase activity (μmol/mg/h)	% Control activity
None (control)	103 ± 4	(100%)
N-acetylimidazole	229 ± 10	220%
N-acetylimidazole, then Triton X-100	7.0 ± 1.5	6.8%
Triton X-100	5.6 ± 0.6	5.4%
Triton X-100, then *N*-acetylimidazole	5.6 ± 0.6	5.4%

Analysis of tertiary structure of the mutants by Cibacron blue binding

To explore the possibility of global misfolding induced by point mutations leading to the inability to bind the nucleotide analogue triazine dye, Cibacron blue, Cibacron blue binding assays were performed as previously described [12]. Misfolded mutants are unable to bind Cibacron blue affinity matrix, as is denatured NTPDase3 (exemplified by the boiled, wild-type enzyme [12]). All the mutants described in this study bound to the Cibacron blue matrix like the wild-type enzyme (data not shown), suggesting that there are no gross changes in tertiary conformations of the mutants affecting the ability to bind the nucleotide analogue, Cibacron blue.

Effect of N-acetylimidazole on Triton X-100 solubilized wild-type NTPDase Mg-ATPase activity

To investigate whether *N*-acetylimidazole can increase Mg^{2+}-ATPase activity of wild-type NTPDase3 after dissociation into monomers by Triton X-100, wild-type NTPDase3 was solubilized with Triton X-100 either prior to, or after, treatment with *N*-acetylimidazole. The results given in Table 3 indicate that *N*-acetylimidazole cannot increase the Mg^{2+}-ATPase activity of Triton X-100 solubilized (monomeric) NTPDase3, and that after *N*-AI is used to increase the activity of the membrane-bound wild-type NTPDase3, that increase in activity is abolished by subsequent Triton X-100 solubilization. Therefore, it appears that the increase in enzyme activity seen upon *N*-acetylimidazole treatment may be dependent on native quaternary structure, or upon the native tertiary structure,

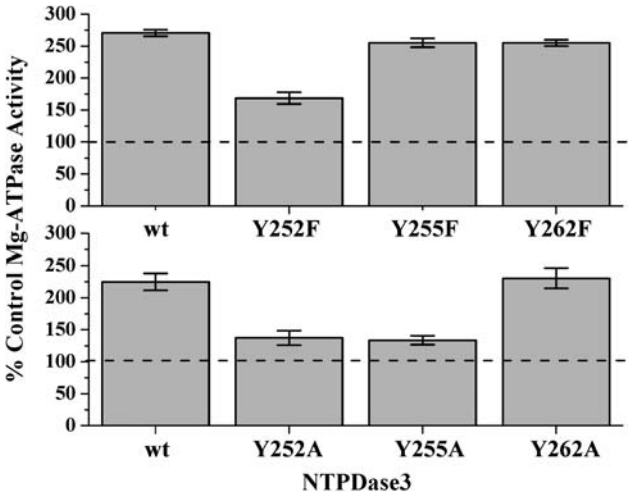

Figure 4. Effect of Concanavalin A pre-treatment on Mg^{2+}-ATPase activities of wild-type and tyrosine mutant NTPDase3. Wild-type and mutant COS cell membranes were pre-incubated with Con A for 15 min at 37 °C prior to addition of ATP to start the reactions as described in Materials and methods. Data shown are the means ± standard deviations for each NTPDase3 sample.

since the native tertiary structure may be modified by disruption of the quaternary structure by Triton X-100.

Effect of Concanavalin A on NTPDase3 wild-type and tyrosine mutants

Concanavalin A is a tetravalent protein that binds to glycans and can stabilize the oligomeric structure of glycoproteins by induction of the formation of protein oligomeric lattices [16]. Concanavalin A was previously shown to increase the nucleotidase activity of several membrane bound, oligomeric NTPDases [18, 22, 37, 38]. The elimination of a single glycosylation site located near ACR1 (N81 in NTPDase3) was shown to greatly diminish the ability of Con A to increase the nucleotidase activity of NTPDase3 [20]. Thus, we used Con A as another probe to determine if the *N*-AI effect may be related to a quaternary structure effect. The data in Figure 4 are consistent with the *N*-acetylimidazole data in Figures 1 and 2, i.e., the mutants which do not respond to *N*-AI also respond less to the stimulating effect of Con A, suggesting some subtle conformational changes in the Y252F, Y252A, and Y255A mutants, which may subtly affect the quaternary structure.

Effect of DSS chemical cross-linking on the nucleotidase activity of tyrosine mutant and wild-type NTPDase3

The lysine specific chemical modification reagent, DSS, was used to treat wild-type and mutant NTPDases to observe the effects on Mg-ATPase activities. As can be seen in the top panel of Figure 5, DSS treatment increased the activity of the wild-type as well as the Y255F and Y262F mutants, but decreased the activity of the Y252F mutant, whose activity is also not stimulated by *N*-acetylimidazole (see Figure 2). In addition, the correlation between stimulation of activity by *N*-AI and by DSS cross-linking also exists for the tyrosine to alanine mutants, since both Y252A and Y255A, which are not stimulated by *N*-AI (see Figure 1), are also not stimulated by DSS cross-linking (bottom panel of Figure 5).

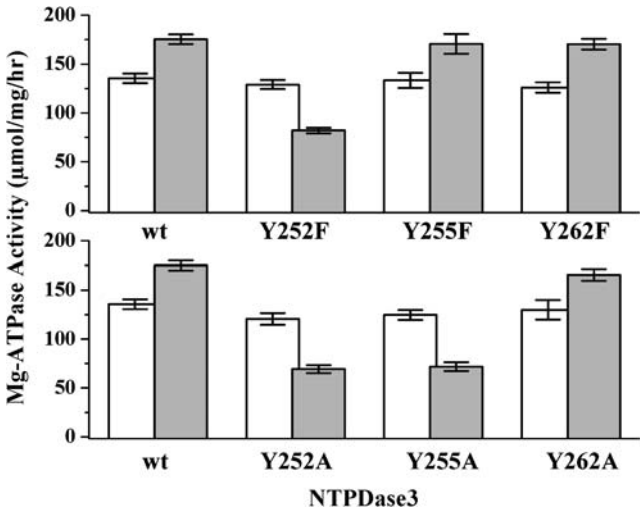

Figure 5. Effect of DSS chemical cross-linking on Mg^{2+}-ATPase activities of wild-type and tyrosine mutant NTPDase3. Wild-type and mutant COS cell membranes were cross-linked with 200 µM DSS for 10 min at 22 °C as described in Materials and methods, the reactions stopped by quenching with excess lysine, and the nucleotidase activities measured. White bars are without DSS cross-linking (controls), while gray bars are NTPDase3 samples after DSS cross-linking. Data shown are the means ± standard deviations for each NTPDase3 sample.

Discussion

In this study we used site-directed mutagenesis to mutate several conserved tyrosines to investigate which tyrosine residue(s) is(are) responsible for mediating the increase in Mg^{2+}-ATPase activity caused by acetylation with the chemical modification reagent, *N*-acetylimidazole (Table 1). These tyrosine residues (see Table 1) are in the vicinity of the glycine residue that was previously proposed to be important for NTPDase3 higher-order structure (due to results obtained upon mutation of glycine 263 in ACR4a [12]), and are also located near the computer-predicted helix–loop–helix dimerization domain [31] of NTPDase3 (^{238}NTSDIMQVS^{246}). These amino acids were first changed to alanine to compare results to our previous studies where NTPDase3 residues were typically mutated to alanine [12, 23, 24, 29, 32]. However, for the purpose of introducing the least structural perturbations and yet allowing us to delineate the residue(s) modified by *N*-acetylimidazole, these tyrosine residues were also mutated to phenylalanine. As can be seen in Table 2, mutation of none of these three tyrosine residues to either alanine or phenylalanine inactivated the enzyme, indicating that they are not an essential part of the catalytic site.

Upon treatment with *N*-acetylimidazole, wild-type NTPDase3 displays a time-dependent increase in Mg^{2+}-ATPase and Mg^{2+}-ADPase activities (see Figures 1 and 2). A substantial portion of the increase in activity is rapidly reversible by hydroxylamine treatment, suggesting that tyrosine modification, rather than lysine modification, is responsible for the effect. The Y252F mutant does not exhibit this *N*-acetylimidazole-induced increase in activity, while the nearby Y255F and Y262F mutants behave like the wild-type enzyme (Figure 2). This suggests that modification (acetylation by *N*-acetylimidazole) of tyrosine at position 252 mediates the effect. However, it is not clear why the increase in activity is not completely reversible with hydroxylamine treatment, if the effect is solely mediated by a single tyrosine acetylation, as the mutagenesis results suggest. Consistent with the phenylalanine mutants, the Y252A mutant is unresponsive to *N*-AI treatment. However, the Y255A mutant, unlike the Y255F mutant, is also largely unresponsive to *N*-AI treatment (Figure 1). The reason for this is not known, but we speculate that the Y255A mutation, being less conservative in nature and introducing a substantially smaller side chain at that position than the Y255F mutation, could cause a perturbation in the folding in that area of the protein, resulting in a microenvironment at Y252 that is either less conducive for the reaction of Y252 with *N*-AI, or alternatively, less conducive

to the change in local conformation that presumably occurs after acetylation of Y252 by *N*-AI.

There are no obvious, global changes in tertiary or quaternary structures in any of the mutants described in this study, since all the mutants have expression levels and enzyme activities not very different from the wild-type enzyme (Table 2). In addition, they all behave like wild-type NTPDase3 in Cibacron blue binding assays, as well as on native gels, and have similar relative susceptibility to intermolecular DSS cross-linking (data not shown since all characteristics were not different from the wild-type).

However, we found that Triton X-100 solubilization abolished the *N*-acetylimidazole-mediated increase in Mg^{2+}-ATPase activity of wild-type NTPDase3, and that monomerization by Triton X-100 solubilization subsequent to stimulation of activity by *N*-AI negates the *N*-AI-induced increase in activity (Table 3). This is important since solubilization with Triton X-100 detergent has been shown to cause a decrease in enzyme activity accompanying disruption of the native oligomeric structure to monomeric enzyme for both NTPDase1 (CD39 [14]) and NTPDase3 [15]. This suggests that the *N*-acetylimidazole-mediated increase in enzyme activity might be associated with a subtle effect on the quaternary structure, which is not detected by the global nature of the DSS cross-linking and native gel analyses. Consistent with this is the fact that the *N*-acetylimidazole induced increase of the ATPase activity is more pronounced than the increase of the ADPase activity (see Figures 1 and 2), since, based on Triton X-100 solubilization (monomerization) experiments, it appears that ATPase activity is more dependent on native quaternary structure than ADPase activity for both NTPDase1 [14] and NTPDase3 [15]. Also consistent with the possibility that the *N*-acetylimidazole-mediated increase in enzyme activity might be associated with a subtle effect on the quaternary structure is the observation that *N*-AI does not increase the activity (data not shown) of bacterially expressed NTPDase6 [39], which is a soluble, monomeric NTPDase that contains the conserved tyrosines corresponding to residues 252 and 255 in NTPDase3 (see Table 1). In addition, there is precedence for *N*-acetylimidazole acetylation of proteins affecting quaternary structure and stability of oligomeric proteins, since Pal et al. reported that this reagent acetylated surface exposed tyrosine residues, resulting in a destabilization of the native subunit assembly of the alpha-crystallin protein [40]. Alternatively, monomerization by Triton X-100 may also modify the native tertiary structure of NTPDase3, and it could be that this alteration in the tertiary structure leads to the observed abolition of the *N*-acetylimidazole-mediated increase in Mg-ATPase activity.

Concanavalin A, a tetravalent ligand known to stabilize the oligomeric structure of glycoproteins by induction of high-order protein oligomer lattice formation [16], increases the nucleotidase activity of several eNTPDases [18, 19, 37, 38, 41–43]. This Con A effect has been previously attributed to stabilization of the native quaternary structure [13, 20]. Thus, we used this lectin as an additional probe of subtle conformational effects of the mutations in this study. The results obtained (see Figure 4) are consistent with, and complementary to, the *N*-AI results in Figures 1 and 2. Thus, mutations in this region that affect the ability of *N*-AI acetylation to increase NTPDase3 enzyme activity, possibly via subtle stabilization of the native quaternary structure, also manifest themselves with regard to the ability of Con A to stimulate enzyme activity. As a result, Con A has a lesser effect on the activity of the Y252F mutant than on the Y255F, Y262F, and wild-type NTPDase3 (Figure 4, top panel).

Chemical cross-linking using the lysine-specific agent, DSS, is also consistent with the *N*-AI and Con A results, since the tyrosine mutants that are unable to respond to *N*-AI also do not respond like the wild-type NTPDase3 to DSS cross-linking with a similar increase in activity (Figure 5). Instead of the increase in activity of the wild-type enzyme, these mutants display reduced activities after lysine-specific cross-linking (DSS treatment). This reduction in activity could be due to reaction at other lysine residues, the negative effect of which is masked in the wild-type enzyme by the larger positive effect on activity after reaction with a different set of lysine residues.

Very recently, Grinthal and Guidotti [44] found that for the related CD39/NTPDase1 protein, the CD39 dimer appears to be in relatively rapid equilibrium with monomeric CD39. Thus, those authors proposed that NTPDase1 exists in a relatively unstable dimeric quaternary structure, which allows exchange of monomer protein partners between different dimers. Since the dimer form of oligomeric NTPDases has higher nucleotidase activity than the monomer form, it follows that any mutation or chemical modification that shifts this monomer–dimer equilibrium more towards the dimer would be expected to increase enzyme activity. Thus, one possible explanation for the *N*-acetylimidazole induced increase in NTPDase3 activity observed in our studies is that acetylation of tyrosine 252 causes a relatively small increase in the stability of the dimer (i.e., slightly shifts the monomer–dimer equilibrium more in favor of the dimer), which is observed as an increase in activity, but is not detected by the relatively crude chemical cross-linking and native gel analyses utilized in this study.

Acknowledgements

We thank Dr Carrie Hicks-Berger for construction of several NTPDase3 tyrosine to alanine mutants. This work was supported by NIH grants HL59915 and HL72882 to T.L.K.

References

1. Zimmermann H, Beaudoin AR, Bollen M et al. Proposed nomenclature for two novel nucleotide hydrolyzing enzyme families expressed on the cell surface. In Vanduffel L (ed): Second

International Workshop on Ecto-ATPases and Related Ectonucleotidases, Maastricht, the Netherlands, 1999–2000. Diepenbeek, Belgium: Shaker Publishing, 1999; 1–9.
2. Braun N, Fengler S, Ebeling C et al. Sequencing, functional expression and characterization of rat NTPDase6, a nucleoside diphosphatase and novel member of the ecto-nucleoside triphosphate diphosphohydrolase family. Biochem J 2000; 351(Pt 3): 639–47.
3. Chadwick BP, Frischauf AM. The CD39-like gene family: Identification of three new human members (CD39L2, CD39L3, and CD39L4), their murine homologues, and a member of the gene family from Drosophila melanogaster. Genomics 1998; 50(3): 357–67.
4. Hicks-Berger CA, Chadwick BP, Frischauf A-M, Kirley TL. Expression and characterization of soluble and membrane-bound human nucleoside triphosphate diphosphohydrolase 6 (CD39L2). J Biol Chem 2000; 275: 34041–5.
5. Yeung G, Mulero JJ, McGowan DW et al. CD39L2, A gene encoding a human nucleoside diphosphatase, predominantly expressed in the heart. Biochemistry 2000; 39(42): 12916–23.
6. Paez JG, Recio JA, Rouzaut A, Notario V. Identity between the PCPH proto-oncogene and the CD39L4 (ENTPD5) ectonucleoside triphosphate diphosphohydrolase gene. Int J Oncol 2001; 19(6): 1249–54.
7. Mulero JJ, Yeung G, Nelken ST et al. Biochemical characterization of CD39L4. Biochemistry 2000; 39(42): 12924–8.
8. Bigonnesse F, Levesque SA, Kukulski F et al. Cloning and characterization of mouse nucleoside triphosphate diphosphohydrolase-8. Biochemistry 2004; 43(18): 5511–9.
9. Handa M, Guidotti G. Purification and cloning of a soluble ATP-diphosphohydrolase (apyrase) from potato tubers (*Solanum tuberosum*). Biochem Biophys Res Commun 1996; 218(3): 916–23.
10. Vasconcelos EG, Ferreira ST, De Carvalho TMU et al. Partial purification and immunohistochemical localization of ATP diphosphohydrolase from *Schistosoma mansoni* – immunological cross-reactivities with potato apyrase and *Toxoplasma gondii* nucleoside triphosphate hydrolase. J Biol Chem 1996; 271(36): 22139–45.
11. Kegel B, Braun N, Heine P et al. An Ecto-ATPase and an Ecto-ATP diphosphohydrolase are expressed in rat brain. Neuropharmacology 1997; 36: 1189–200.
12. Kirley TL, Yang F, Ivanenkov VV. Site-directed mutagenesis of human nucleoside triphosphate diphosphohydrolase 3: The importance of conserved glycine residues and the identification of additional conserved protein motifs in eNTPDases. Arch Biochem Biophys 2001; 395(1): 94–102.
13. Stout JG, Kirley TL. Control of cell membrane ecto-ATPase by oligomerization state: Intermolecular cross-linking modulates ATPase activity. Biochemistry 1996; 35(25): 8289–98.
14. Wang T-F, Ou Y, Guidotti G. The transmembrane domains of ectoapyrase (CD39) affect its enzymatic activity and quaternary structure. J Biol Chem 1998; 273(38): 24814–21.
15. Murphy DM, Ivanenkov VV, Kirley TL. Identification of cysteine residues responsible for oxidative cross-linking and chemical inhibition of human nucleoside triphosphate diphosphohydrolase 3. J Biol Chem 2002; 277: 6162–9.
16. Mandal DK, Brewer CF. Interactions of Concanavalin A with glycoproteins: Formation of homogenous glycoprotein–lectin cross-linked complexes in mixed precipitation systems. Biochemistry 1992; 31: 12602–9.
17. Kirley TL, Stout JG. Purification, characterization, and molecular cloning of the chicken gizzard smooth muscle ecto-ATPase. In Plesner L, Kirley TL, Knowles AF (eds): Ecto-ATPases: Recent Progress on Structure and Function. New York: Plenum Press 1997; 111–26.
18. Megias A, Martinez-Senac MM, Delgado J, Saborido A. Regulation of transverse tubule ecto-ATPase activity in chicken skeletal muscle. Biochem J 2001; 353: 521–9.
19. Caldwell CC, Hornyak SC, Pendleton E et al. Regulation of chicken gizzard ecto-ATPase activity by modulators that affect its oligomerization status. Arch Biochem Biophys 2001; 387(1): 107–16.
20. Murphy DM, Kirley TL. Asparagine 81, an invariant glycosylation site near apyrase conserved region 1, is essential for full enzymatic activity of ecto nucleoside triphosphate diphosphohydrolase 3. Arch Biochem Biophys 2003; 413(1): 107–15.
21. Smith TM, Kirley TL. Glycosylation is essential for functional expression of a human brain ecto-apyrase. Biochemistry 1999; 38(5): 1509–16.
22. Hicks-Berger CA, Kirley TL. Expression and characterization of human Ecto-ATPase and chimeras with CD39 ecto-apyrase. IUBMB Life 2000; 50: 43–50.
23. Yang F, Hicks-Berger CA, Smith TM, Kirley TL. Site-directed mutagenesis of human nucleoside triphosphate diphosphohydrolase 3: The importance of residues in the apyrase conserved regions. Biochemistry 2001; 40(13): 3943–50.
24. Hicks-Berger CA, Yang F, Smith TM, Kirley TL. The importance of histidine residues in human ecto-nucleoside triphosphate diphoshohydrolase-3 as determined by site-directed mutagenesis. Biochim Biophys Acta 2001; 1547: 72–81.
25. Small DAP, Lowe CR, Atkinson T, Bruton CJ. Affinity labelling of enzymes with triazine dyes. Eur J Biochem 1982; 128: 119–23.
26. Witt JJ, Roskoski R. Adenosine cyclic 3′,5′-monophosphate dependent protein kinase: Active site inhibition by cibacron blue F3GA. Biochemistry 1980; 19: 143–8.
27. Stout JG, Kirley TL. Inhibition of purified chicken gizzard ecto-ATPase by P2 purinoceptor antagonists. Biochem Mol Biol Int 1995; 36: 927–34.
28. Chen BC, Lee CM, Lin WW. Inhibition of ecto-ATPase by PPADS, suramin and reactive blue in endothelial cells, C6 glioma cells and RAW 264.7 macrophages. Br J Pharmacol 1996; 119(8): 1628–34.
29. Smith TM, Lewis Carl SA, Kirley TL. Mutagenesis of two conserved tryptophan residues of the E-type ATPases: Inactivation and conversion of an ecto-apyrase to an ecto-NTPase. Biochemistry 1999; 38: 5849–57.
30. Buffon A, Ribeiro VB, Furstenau CR et al. Acetylsalicylic acid inhibits ATP diphosphohydrolase activity by platelets from adult rats. Clin Chim Acta 2004; 349(1–2): 53–60.
31. Murre C, McCaw PS, Baltimore D. A new DNA binding and dimerization motif in immunoglobulin enhancer binding, daughterless, MyoD, and myc proteins. Cell 1989; 56(5): 777–83.
32. Smith TM, Kirley TL. Site-directed mutagenesis of a human brain ecto-apyrase: Evidence that the E-type ATPases are related to the actin/heat shock 70/sugar kinase superfamily. Biochemistry 1999; 38(1): 321–8.
33. Stoscheck CM. Increased uniformity in the response of the Coomassie blue G protein assay to different proteins. Anal Biochem (1990) 184: 111–6.
34. Fiske CH, Subbarow Y. The colorometric determination of phosphorous. J Biol Chem 1925; 66: 375–400.
35. Schwartz A, Allen JC, Haragaya S. Possible involvement of cardiac Na^+,K^+-ATPase in the mechanism of action of cardiac glycosides. J Pharmacol Exp Ther 1969; 168: 31–41.
36. Baykov AA, Evtushenko OA, Avaeva SM. A malachite green procedure for orthophosphate determination and its use in alkaline phosphatase-based enzyme immunoassay. Anal Biochem 1988; 171(2): 266–70.
37. Moulton MP, Sabbadini RA, Norton KC, Dahms AS. Studies on the transverse tubule Mg-ATPase-lectin induced alterations of kinetic behavior. J Biol Chem 1986; 261: 12244–51.
38. Stout JG, Kirley TL. Purification and characterization of the ecto-Mg-ATPase of chicken gizzard smooth muscle. J Biochem Biophys Methods 1994; 29(1): 61–75.
39. Ivanenkov VV, Murphy-Piedmonte DM, Kirley TL. Bacterial expression, characterization, and disulfide bond determination of soluble human NTPDase6 (CD39L2) nucleotidase: Implications for structure and function. Biochemistry 2003; 42(40): 11726–35.
40. Pal JK, Bera SK, Ghosh SK. Acetylation of alpha-crystallin with *N*-acetylimidazole and its influence upon the native aggregate and subunit reassembly. Curr Eye Res 1999; 19(4): 358–67.

41. Beeler T, Gable KS, Keffer JM. Characterization of the membrane bound Mg^{2+}-ATPase of rat skeletal muscle. Biochim Biophys Acta 1983; 734: 221–34.
42. Kirley TL, Gerber LK, Smith TM. Expression and characterization of chicken muscle ecto-ATPase in mammalian COS cells. IUBMB Life 1999; 48: 67–72.
43. Marcus AJ, Broekman MJ, Drosopoulos JH et al. The endothelial cell ecto-ADPase responsible for inhibition of platelet function is CD39. J Clin Invest 1997; 99(6): 1351–60.
44. Grinthal A, Guidotti G. Dynamic motions of CD39 transmembrane domains regulate and are regulated by the enzymatic active site. Biochemistry 2004; 43(43): 13849–58.